

# Two-dimensional model of dynamical fermion mass generation in strongly coupled gauge theories

W. Franzki<sup>1,2,3</sup>,  
J. Jersák<sup>1,2,4</sup>, and R. Welters<sup>1,2,5</sup>

<sup>1</sup>*Institute of Theoretical Physics E, RWTH Aachen, D-52056 Aachen, Germany*

<sup>2</sup>*HLRZ c/o KFA Jülich, D-52425 Jülich, Germany*

## Abstract

We generalize the  $N_F = 2$  Schwinger model on the lattice by adding a charged scalar field. In this so-called  $\chi U \phi_2$  model the scalar field shields the fermion charge, and a neutral fermion, acquiring mass dynamically, is present in the spectrum. We study numerically the mass of this fermion at various large fixed values of the gauge coupling by varying the effective four-fermion coupling, and find an indication that its scaling behavior is the same as that of the fermion mass in the chiral Gross-Neveu model. This suggests that the  $\chi U \phi_2$  model is in the same universality class as the Gross-Neveu model, and thus renormalizable and asymptotic free at arbitrary strong gauge coupling.

<sup>3</sup> E-mail address: wfranzki@hrz.kfa-juelich.de

<sup>4</sup> E-mail address: jersak@physik.rwth-aachen.de

<sup>5</sup> Present address: AMS, Am Seestern 1, 40547 Düsseldorf

# 1 Introduction

Strongly coupled gauge theories tend to break dynamically chiral symmetry, but fermions which acquire mass through this mechanism are usually confined, as it is the case in the Schwinger model or in the QCD. From the point of view of the electroweak symmetry breaking in, or beyond the standard model, a dynamical mass generation without the fermion confinement is of interest. Such a situation arises in a class of chiral symmetric strongly coupled gauge theories on the lattice, in which the gauge charge of the fermion acquiring mass dynamically is shielded by a scalar field of the same charge[1]. The question is whether such models are renormalizable at strong gauge coupling, so that the lattice cutoff can be removed, and the resulting field theory might be applicable in continuum.

In this work we consider such a lattice model with U(1) chiral symmetry and vectorlike U(1) gauge symmetry, the  $\chi U\phi_d$  model, in  $d = 2$  dimensions. It consists of a staggered fermion field  $\chi$ , a gauge field  $U \in U(1)$  living on the lattice links of length  $a$ , and a complex scalar field  $\phi$  with frozen length  $|\phi| = 1$ . The unconfined fermion field is  $F = \phi^\dagger \chi$ . There is no Yukawa coupling, and the mass  $am_F$  of the fermion  $F$  arises dynamically. Because of the fermion doubling the fermion number is  $N_F = 2$ . The  $\chi U\phi_2$  model can be seen either as a generalization of the Schwinger model with  $N_F = 2$  by adding a charged scalar field, or as the 2D scalar QED with added fermions. Similar models have been studied nearly 20 years ago in the context of the instanton investigations [2].

The four dimensional  $\chi U\phi_4$  model, considered as a possible theory with dynamical mass generation of unconfined fermions [1], has been investigated recently. In spite of some encouraging results [3, 4] a clarification of its renormalizability properties remains a difficult task. Here we demonstrate that in a simpler case, in 2 dimensions, these properties can be investigated with remarkable clarity. Within the limits of numerical accuracy, we find that the  $\chi U\phi_2$  model is renormalizable at strong gauge coupling  $g$ , because it belongs to the universality class of the two-dimensional chiral Gross-Neveu (GN<sub>2</sub>) model with  $N_F = 2$ .

The GN<sub>2</sub> model is known to generate fermion mass dynamically at arbitrarily weak four-fermion coupling  $G$ , to be nonperturbatively renormalizable, and asymptotically free. One of its lattice regularizations is identical to the  $\chi U\phi_2$  model in the limit of infinite gauge coupling,  $\beta = 1/a^2 g^2 = 0$ . In this limit the four-fermion coupling  $G$  is an invertible function  $G(\kappa)$  of the hopping parameter  $\kappa$  of the scalar field  $\phi$  (or, equivalently, of its bare mass) in the  $\chi U\phi_2$  model, with  $G(\kappa) \rightarrow 0$  as  $\kappa \rightarrow \infty$ . The scaling behavior associated with the asymptotic freedom, and the continuum limit of the GN<sub>2</sub> model, are thus obtained as  $\kappa \rightarrow \infty$ .

These are extremely useful facts when the  $\chi U\phi_2$  model is investigated at a finite gauge coupling, i. e., at nonvanishing  $\beta$ . The idea is to compare the scaling behavior of the  $\chi U\phi_2$  model with that of the GN<sub>2</sub> model, as  $\kappa$  grows at fixed  $\beta > 0$ . For this purpose we introduce an effective four-fermion coupling  $\tilde{G}(\beta, G)$ . This is now a coupling of the “composite” fermions  $F = \phi^\dagger \chi$ , and thus characterizes the van der Waals forces arising from the fundamental interactions between the fields. At  $\beta = 0$  it coincides with the GN<sub>2</sub> coupling,  $\tilde{G}(0, G) = G$ . For  $\beta > 0$ ,  $\tilde{G}$  is smaller than  $G$ , but depends on  $\kappa$  similarly as  $G(\kappa)$ . For the comparison it is therefore convenient to use  $G$  instead of  $\kappa$  as one argument of  $\tilde{G}$ . We investigate the scaling behavior of  $am_F$  with decreasing  $\tilde{G}(\beta, G)$  at various fixed  $\beta > 0$ , and compare it with the  $\beta = 0$  case.

A determination of  $\tilde{G}(\kappa, \beta)$  directly by means of the four-point function of the composite field would be very expensive. Instead, we introduce it in an indirect way: we make the assumption that the scaling behavior of  $am_F$  in the  $\chi U\phi_2$  model at  $\beta > 0$  is described by the truncated Schwinger-Dyson (SD) equations of the same structure as at  $\beta = 0$  in the GN<sub>2</sub>

model. The only change is the replacement of  $G$  by  $\tilde{G}(G, \beta)$ . Our numerical study of the  $\chi U\phi_2$  model at  $\beta > 0$  is mainly concerned with the verification of this assumption.

The use of the SD equations serves further purposes. One is to provide an analytic framework in which the numerical results obtained at small but nonzero bare fermion mass  $am_0$  can be related to the chiral limit case,  $m_0 = 0$ , we are actually interested in. Simulations at  $m_0 = 0$  are too time consuming on larger lattices, and the scaling behavior has to be studied at  $am_0 > 0$  by varying both  $G$  and  $am_0$ . The SD equations suggest how to vary both parameters simultaneously, approaching the critical point,  $G = am_0 = 0$ , and how to extrapolate to the chiral limit  $m_0 = 0$ . We test this strategy carefully at  $\beta = 0$ , exploiting the knowledge of the chiral limit there, and find it remarkably successful. Small deviations, not accounted for by the SD equations within the used truncation scheme, and present at very small  $am_0$ , do not influence the correct scaling behavior following from the asymptotic freedom.

Further benefit of the use of SD equations is the control of the finite size effects. Following Ref. [5], we solve these equations on lattices of the same sizes and boundary conditions as those on which numerical data are obtained. This allows a suitable choice of the data points in the parameter space, as well as an extrapolation to the infinite volume limit.

Finally, the SD equations allow us to describe the preasymptotic behavior of the data, obtained for correlation lengths limited by the lattice size, and to infer the genuine scaling behavior for diverging correlation length. At  $\beta = 0$ , we have verified that when the SD equations are used for the extrapolation, then from those data the correct scaling behavior with  $G \rightarrow 0$  is obtained.

We find that in the  $\chi U\phi_2$  model with  $\beta \leq 1$  the preasymptotic behavior, and thus presumably also the scaling behavior of the fermion mass  $am_F$  is described quite well by the same SD equations as in the chiral  $\text{GN}_2$  model, now with  $\tilde{G}(\beta, G)$  replacing  $G$ . The same scaling behavior as in the  $\text{GN}_2$  model is indicated, with  $\tilde{G} \rightarrow 0$  as  $\kappa \rightarrow \infty$ .

On the basis of this evidence we suggest that the  $\chi U\phi_2$  model belongs, along the critical line at  $\kappa = \infty$ , to the same universality class as the  $\text{GN}_2$  model, and is thus nonperturbatively renormalizable. The  $\chi U\phi_2$  model is therefore an example of a renormalizable quantum field theory in which the fermion mass is generated dynamically at strong gauge coupling by the shielded gauge mechanism suggested in Ref. [1].

In the following section we define the  $\chi U\phi_2$  model and explain its relationship to the  $\text{GN}_2$  model at  $\beta = 0$ . In Sec. 3 the phase diagram is described. The SD equations, and also the determination of the effective four-fermion coupling  $\tilde{G}(\beta, G)$  by means of their inversion, are discussed in Sec. 4. In the Sec. 5 we test these equations, and the accuracy of determination of  $\tilde{G}$  at  $\beta = 0$ . In Sec. 6 we then apply the same method of analysis to the data for  $am_F$  at  $0 < \beta \leq 1$ , demonstrate the applicability of the same SD equations as at  $\beta = 0$ , and determine  $\tilde{G}(\beta, G)$ . The scaling behavior of the data is illustrated in Sec. 7. We conclude in Sec. 8 with some remarks about the meaning of our results.

## 2 The $\chi U\phi_2$ model and its $\text{GN}_2$ limit

The action of the  $\chi U\phi_2$  model consists of three parts:

$$S_{\chi U\phi} = S_\chi + S_U + S_\phi, \quad (2.1)$$

where

$$S_\chi = \frac{1}{2} \sum_x \bar{\chi}_x \sum_{\mu=1}^2 \eta_{x\mu} (U_{x,\mu} \chi_{x+\mu} - U_{x-\mu,\mu}^\dagger \chi_{x-\mu}) + am_0 \sum_x \bar{\chi}_x \chi_x,$$

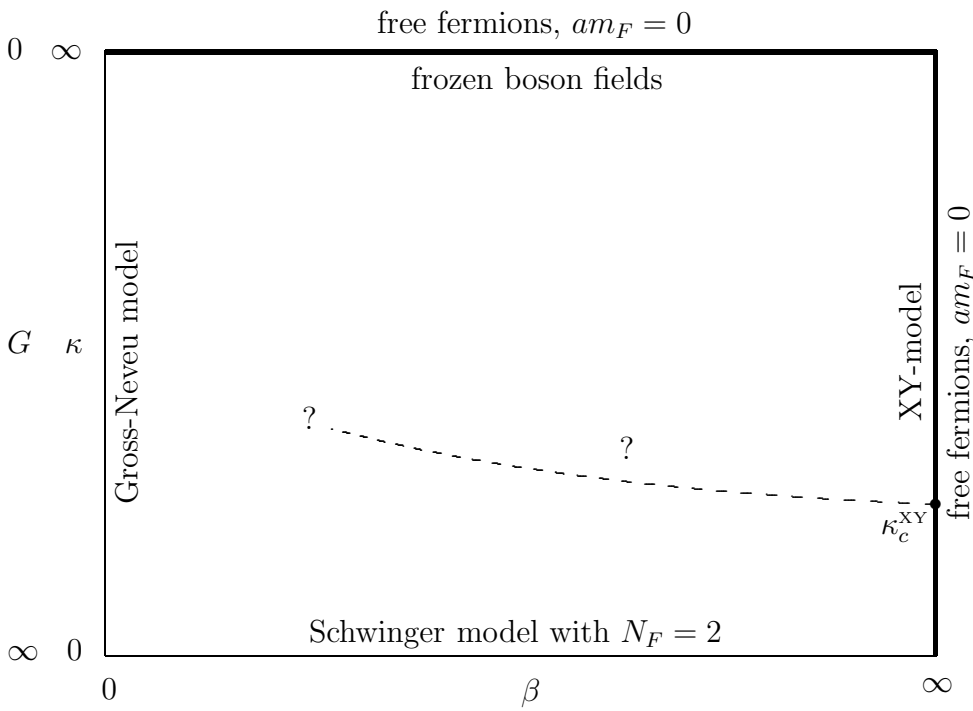


**Figure 1:** Phase diagram of the  $\chi U \phi_2$  model for  $m_0 = 0$ . The well understood limit cases are described. The dashed line indicates a possible topological phase transition. The fermion mass  $am_F$  is nonzero everywhere except on the bold-marked boundaries.

$$S_U = \beta \sum_P (1 - \text{Re } U_P),$$

$$S_\phi = -\kappa \sum_x \sum_{\mu=1}^2 (\phi_x^\dagger U_{x,\mu} \phi_{x+\mu} + h.c.).$$

Here,  $x$  and  $x + \mu$  denote lattice sites and their nearest neighbors, respectively, and  $\chi$  is a staggered fermion field,  $\eta_{x\mu}$  being the usual phase factors. The link variables  $U_{x,\mu} \in \text{U}(1)$  represent a compact abelian gauge field with coupling  $\beta = 1/a^2 g^2$ , and  $\phi$  is a complex scalar field with the constraint  $|\phi_x| = 1$ . The fermion and scalar fields have the same unit charge. The bare fermion mass  $m_0$  is introduced for technical reasons, and we are interested in the limit  $m_0 = 0$ , where the action has a global  $\text{U}(1)$  chiral symmetry. The phase diagram of this model is shown in Fig. 1.

In the limit case  $\beta = 0$ , one can perform the Lee-Shrock transformation [6], in which the scalar and gauge fields are integrated out and a four-fermion term appears. This leads to the action

$$S_{4f} = -\sum_x \sum_{\mu=1}^2 \left( G \bar{\chi}_x \chi_x \bar{\chi}_{x+\mu} \chi_{x+\mu} - \frac{1}{2} \eta_{x\mu} [\bar{\chi}_x \chi_{x+\mu} - \bar{\chi}_{x+\mu} \chi_x] \right) + \frac{am_0}{r} \sum_x \bar{\chi}_x \chi_x, \quad (2.2)$$

with

$$G = G(\kappa) = \frac{1 - r^2}{4r^2} \quad (2.3)$$

and

$$r = \frac{I_1(2\kappa)}{I_0(2\kappa)}. \quad (2.4)$$

For  $m_0 = 0$  the transformed action (2.2) is that of the chiral  $\text{GN}_2$  model in a certain lattice regularization. Within the uncertainty of interpretation of a continuum limit of staggered fermions with a strong gauge coupling it can be possibly interpreted also as a

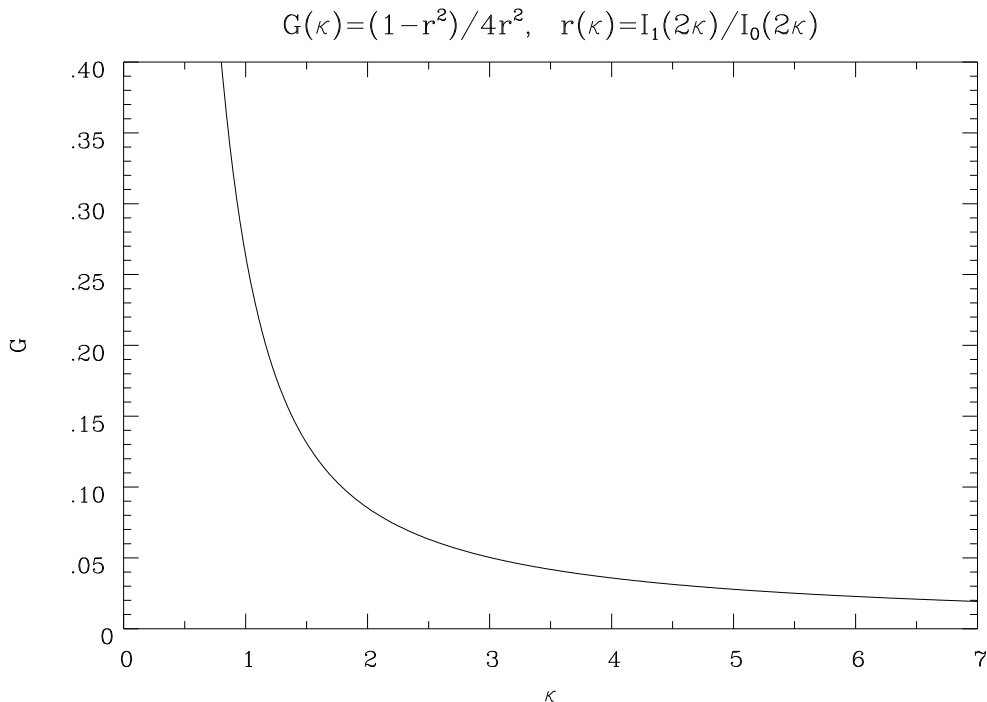


**Figure 2:** Relation between the four fermion coupling  $G$  and  $\kappa$  at  $\beta = 0$ .

lattice formulation of the Thirring model [7]. The  $\text{GN}_2$  model has a critical point at  $G = 0$ , where the fermion mass vanishes like

$$am_F \underset{G \rightarrow 0}{\propto} e^{-\frac{\pi}{8G}}. \quad (2.5)$$

The four fermion coupling  $G(\kappa)$  is a function of  $\kappa$  shown in Fig. 2. From the point of view of the scaling behavior (2.5), the use of  $G(\kappa)$  as a parameter instead of  $\kappa$  is very convenient, and we therefore adopt such a reparametrization even at  $\beta > 0$ . There  $G$  is not a four-fermion coupling any more, it only replaces the hopping parameter  $\kappa$  according to eq. (2.3). Also  $r$ , eq. (2.4), will be understood as a function of  $G$  from now on, satisfying  $r(G) \rightarrow 1$  as  $G \rightarrow 0$ .

We note that the bare mass  $am_0/r$  in the action (2.2) of the  $\text{GN}_2$  model is different from that of the  $\chi U\phi_2$  model (2.1), as the field  $\chi$  has been rescaled by  $\sqrt{r}$  in the course of the Lee-Shrock transformation. We use  $am_0$  of the  $\chi U\phi_2$  model, and the bare mass in the SD equations for the  $\text{GN}_2$  model is therefore slightly  $G$ -dependent at fixed  $am_0$ .

We perform the hybrid Monte Carlo simulations on the  $V = L^2$  lattices, with periodic and antiperiodic boundary conditions in first and second ( $\mu = t$ ) directions, respectively. The fermion mass  $am_F$  is obtained from the gauge invariant propagator  $\langle \phi_x^\dagger \chi_x \phi_y \bar{\chi}_y \rangle$  by inverting the fermion matrix  $M$  and calculating

$$P_{AB}(k) \Big|_{\vec{k}=0} = \frac{1}{V} \sum_{x,y} e^{i(k + \pi_A)x} \phi_x M_{xy}^{-1} \phi_y^\dagger e^{-i(k + \pi_B)y} \Big|_{\vec{k}=0}. \quad (2.6)$$

Here  $\pi_A$  denotes the usual momentum shifts in the Brillouin zone. The mass  $am_F$ , and also the fermion renormalization constant  $Z$  result from the fit in momentum space to

$$\text{Tr} \Gamma_t P(k_t) = Z \frac{-4i \sin k_t}{\sin^2 k_t + (am_F)^2}, \quad (2.7)$$

where  $\Gamma_t$  is the Goltermann-Smit matrix  $(\Gamma_{\mu=t})_{AB}$ . This procedure is chiral invariant.

### 3 Other limit cases and the phase diagram

The schematic phase diagram for  $m_0 = 0$  is shown in Fig. 1. At  $\kappa = 0$ , when the scalar field is decoupled, the  $\chi U\phi_2$  model with  $m_0 = 0$  reduces to the lattice regularized Schwinger model ( $d = 2$  QED) with  $N_F = 2$ . As is well known, this model is anomaly free, confines fermions at all  $\beta < \infty$ , and possesses only massive bosonic states. Thus  $am_F \rightarrow \infty$  as  $\kappa \rightarrow 0$ . The continuum limit is expected at the UV fixed point at  $\beta = \infty$ , and there is no critical point at  $\beta < \infty$ .

At  $\kappa = \infty$ , both the scalar and the gauge fields are frozen.<sup>1</sup> As is seen in the unitary gauge, the fermion field is decoupled, and  $am_F = am_0$ . At  $am_0 = 0$ , the line  $\kappa = \infty$  is thus a critical line at which the fermion mass  $am_F$  vanishes. The  $\beta = 0$  point of this line is the critical point of the GN<sub>2</sub> model.

In the limit  $\beta = \infty$ , when the gauge coupling vanishes, the fermion field is decoupled again, and  $am_F = am_0$ . Thus, in the chiral limit, the line  $\beta = \infty$  is a critical line with vanishing fermion mass, too. The scalar field variables can be seen as spin variables, and the corresponding two-dimensional XY<sub>2</sub> model is known to have a topological phase transition at  $\kappa = \kappa_c^{XY} \simeq 0.56$ .

Let us now consider the inside of the phase diagram in Fig. 1. Old investigations suggest that the model possesses a massive fermion in some parameter region accessible to the dilute instanton gas [2]. As follows from the convergence of the strong coupling expansion, at small nonvanishing  $\beta$ , the model should have the same properties as at  $\beta = 0$ . This implies analyticity and nonvanishing  $am_F$  for  $\kappa < \infty$  at small  $\beta$ .

The fate of the topological transition at  $\beta = \infty$ , as  $\beta$  gets finite, is not completely clear. We have investigated numerically the spectrum of the model in the vicinity of the dashed line shown in Fig. 1. This line is observable at large  $\beta$  as a shallow dip in the masses of the scalar and vector bosons, which can be constructed from the gauge invariant products of the type  $\phi_x^\dagger U_{x,\mu} \phi_{x+\mu}$ . But  $am_F$  shows no sensitivity when the dashed line is crossed, and we have found no state, neither bosonic nor fermionic, indicating a vanishing of the mass in lattice units on this line at  $\beta < \infty$ . The dynamical fermion mass generation at  $\beta < \infty$  is thus not influenced by the remnant of the Kosterlitz-Thoules transition. Presumably, a critical behavior on this remnant, if any, appears only in some topologically nontrivial observables [8]. The mass  $am_F$  stays finite, and the fermion  $F$  gets infinitely heavy in physical units in any conceivable continuum limit taken on this line at  $\beta < \infty$ .

We have checked that there is no indication of any other phase transition, not even of some change of behavior of some local observable, anywhere else in the phase diagram of the  $\chi U\phi_2$  model. Our data thus indicate that the fermion mass  $am_F$  is nonzero for any finite  $\beta$  and  $\kappa$ . It decreases when any of these parameters increases and one of the boundaries bold-marked in Fig. 1 is approached. As in the GN<sub>2</sub> model, the fermion mass generation takes place without the spontaneous chiral symmetry breaking, which is forbidden by the Mermin-Wagner-Coleman Theorem. A continuum limit taken on the line  $\beta = \infty$  might lead to an interesting generalization of the Schwinger model in the continuum. In this work, we concentrate on the scaling behavior of  $am_F$  when the line  $\kappa = \infty$  is approached.

---

<sup>1</sup> This is meant in a sense avoiding the Mermin-Wagner-Coleman theorem: the limit  $\kappa \rightarrow \infty$  is taken before an external “magnetic” field, required for a definition of the spontaneous symmetry breaking, is switched off. We thank G. Roepstorff for a discussion on this point.

## 4 Schwinger-Dyson equations for the GN<sub>2</sub> model

The SD equations for the fermion propagator in a four-fermion theory, truncated after O( $G$ ), can be represented graphically as

$$\begin{aligned}
 \text{---} \bullet \text{---} &= \text{---} \text{---} + \text{---} \text{---} \text{---} \bullet \text{---} + \text{---} \text{---} \text{---} \bullet \text{---} . \\
 & \hspace{15em} (a) \hspace{15em} (b)
 \end{aligned}$$

(4.1)

On a finite lattice they read (see e. g. [5]):

$$N = \frac{am_0}{r(G)} + \frac{4G}{V} \sum_k \frac{N}{\sum_\nu F_\nu^2 (\sin(k_\nu a))^2 + N^2} , \quad (4.2)$$

$$F_\mu = 1 + \frac{2G}{V} \sum_k \frac{F_\mu (\sin(k_\mu a))^2}{\sum_\nu F_\nu^2 (\sin(k_\nu a))^2 + N^2} . \quad (4.3)$$

These are three coupled equations for  $N$  and  $F_\mu$  which we solve numerically. Then

$$am_F = N/F_t , \quad (4.4)$$

$$Z = \frac{1}{rF_t} \quad (4.5)$$

are determined. If the term (b) in (4.1) is neglected, one obtains the gap equation with  $F_\mu = 1$  and  $am_F = N$ .

In the infinite volume, when  $F_1 = F_2 = F$ , and for small  $G$ , the approximate analytic solution of the SD equations is

$$N = \frac{am_0}{r} - \frac{8GN}{\pi F^2} \ln \left( \frac{2N}{\pi F} \right) , \quad (4.6)$$

$$F = \frac{1}{2} + \frac{1}{2} \sqrt{1 + G} . \quad (4.7)$$

For  $m_0 = 0$ , one obtains the scaling behavior (2.5) as  $G \rightarrow 0$ .

The idea of the combined limit  $G \rightarrow 0$  and  $am_0 \rightarrow 0$  is to make  $am_0/r$  a function of  $G$  in such a way that eq. (4.6) is solvable, and that  $am_0(G) \rightarrow 0$  as  $G \rightarrow 0$ . We choose

$$\frac{am_0(G, s)}{r(G)} = (1 - s) \frac{\pi F}{2} e^{-\frac{\pi F^2 s}{8G}} , \quad (4.8)$$

using the approximate solution (4.7) for  $F$ . Here  $s$  is a free parameter obeying  $0 < s \leq 1$ . For this choice of  $am_0$  the solution of eq. (4.6) is

$$N = \frac{\pi F}{2} e^{-\frac{\pi F^2 s}{8G}} , \quad (4.9)$$

and thus

$$am_F = \frac{N}{F} = \frac{\pi}{2} e^{-\frac{\pi F^2 s}{8G}}. \quad (4.10)$$

The asymptotic scaling law along the lines of constant  $s$  is

$$am_F = \frac{\pi}{2} e^{-\frac{\pi s}{8G}}, \quad (4.11)$$

$$\frac{am_F}{am_0} = \frac{1}{1-s}, \quad (4.12)$$

where we have used  $rF \rightarrow 1$  as  $G \rightarrow 0$ . Obviously, the ratio  $m_0/m_F$  does not vanish except if  $s = 1$ . For  $s < 1$ , a continuum GN<sub>2</sub> model with nonvanishing bare mass is obtained. We therefore distinguish between the chiral limit,  $m_0 = 0$  for any  $a$ , and the statement  $am_0 = 0$ , which at a critical point with  $am_F = 0$  allows  $a = 0$ ,  $m_0/m_F \neq 0$ .

It may appear strange that the scaling behavior (4.11) depends on  $s$ , i.e. on the path, though the same critical point is approached. But this is similar to the scaling behavior in a magnetic system described by the equation of state

$$h = M^\delta f\left(\frac{t}{M^{1/\beta}}\right), \quad (4.13)$$

when the external field  $h$  (corresponding to  $am_0/r$ ) and the reduced temperature  $t$  (corresponding to  $G$ ) are varied simultaneously. For example, if

$$h = c \cdot t^p, \quad p \leq \beta\delta, \quad (4.14)$$

the scaling law is  $p$ -dependent,

$$M \propto t^{p/\delta}. \quad (4.15)$$

In our case the scaling is described by an essential singularity instead of the power law (4.15). Needless to say, the SD equations reproduce correctly the first coefficient of the  $\beta$ -function of the GN<sub>2</sub> model with nonvanishing bare mass since the one loop contribution is taken into account correctly.

The truncated SD equations cannot be expected to describe the data correctly at very small  $am_0$ , because the contributions of the neglected fermion loops increase with decreasing  $am_0$ . Then only the exponential scaling behavior, eq. (4.11), but not the value of the constant prefactor in (4.11), and thus of the ratio (4.12), are predicted correctly. We shall take this discrepancy into account by relying in our determination of  $\tilde{G}$  in Sec. 6 on the results at larger values of  $am_0$  (mostly  $am_0 = 0.4$ ).

An important step in our data analysis at  $\beta > 0$  is the use of the inverse SD equations. For a chosen  $\beta$ ,  $s$  and  $am_0$ , the fermion mass  $am_F$ , obtained on a certain lattice, is inserted into the corresponding SD equations (4.2), (4.3) by using eq. (4.4). The four fermion coupling is considered as a free parameter  $\Gamma$ . It is determined by solving the three equations (4.2), (4.3), taken as equations determining  $\Gamma$  and  $F_\mu$ :

$$am_F F_t = \frac{am_0}{r(\Gamma)} + \frac{4\Gamma}{V} \sum_k \frac{am_F F_t}{\sum_\nu F_\nu^2 (\sin(k_\nu a))^2 + (am_F F_t)^2}, \quad (4.16)$$

$$F_\mu = 1 + \frac{2\Gamma}{V} \sum_k \frac{F_\mu (\sin(k_\mu a))^2}{\sum_\nu F_\nu^2 (\sin(k_\nu a))^2 + (am_F F_t)^2}. \quad (4.17)$$

The resulting values of  $\Gamma$  can, in principle, depend on all the parameters,  $\Gamma = \Gamma(\beta, G, am_0, V)$ .



## 5 Test of the SD equations in the $\text{GN}_2$ limit

The aim of this section is to investigate how the known scaling behavior (2.5) of the  $\text{GN}_2$  model can be confirmed by the data for  $am_F$  obtained in numerical simulation of the  $\chi U\phi_2$  model at  $\beta = 0$ . The fermion matrix inversion has turned out to be very slow at  $m_0 = 0$  on large lattices ( $\geq 32^2$ ), and the simulations have to be performed at finite  $am_0$ . We have made several attempts to extrapolate to  $m_0 = 0$  the values of  $am_F$  obtained for several  $am_0$  at fixed  $G$ . However, using e.g. a power law we failed to reproduce reliably the values obtained by long simulations directly at  $m_0 = 0$ .

Therefore we have adopted the strategy of the combined approach to the critical point  $G = am_0 = 0$ , in which  $G$  and  $am_0$  vary simultaneously, choosing the paths  $s = \text{const}$ , eq. (4.8), suggested by the SD equations. The chosen values of  $s$  are  $s = 0.2, 0.3, \dots, 0.7$ . The simulations have been performed at the values of  $am_0$  and  $G$  satisfying the relation (4.8), and chosen such that the value of  $am_F$  predicted by the SD equations satisfies

$$\frac{1}{am_F} < \frac{L}{4}. \quad (5.1)$$

This restriction turned out to be necessary in order to avoid a finite size dependence both of the predicted and measured values of  $am_F$ .

In Fig. 3 we show the semi-logarithmic plot of the data for  $am_F$  against  $1/G$ , and compare them with the prediction of the SD equations (4.2) and (4.3) on the  $32^2$  and  $64^2$  lattices. It demonstrates that the SD equations describe the data for smaller  $s$  very well, and for larger  $s$ ,  $s = 0.6, 0.7$ , still quite well, though for these  $s$  the bare mass is very small. But one cannot see that the data is still far from the asymptotic scaling behavior (4.11), and that the seemingly linear decrease does not have the right slope. Also the size of the error bars is barely visible on the logarithmic scale.

Therefore, in Fig. 4 we show the data as ratios  $am_F/am_0$  plotted on the linear scale. The curves are the SD predictions for this ratio on the  $32^2$  and  $64^2$  lattices (full lines) and  $1024^2$  lattice (dotted lines), whereas the dashed horizontal lines represent the expected asymptotic scaling behavior, eq. (4.12). The benefits of the SD equations become manifest: For smaller  $s$  the agreement with the data is within the tiny but now visible error bars. With increasing  $s$  the agreement gets worse, as expected for decreasing  $am_0$ . Nevertheless, the SD equations still reproduce the  $1/G$ -dependence qualitatively. They predict the onset of finite size effects, manifested by a downward bend of the curves. These effects set on at larger  $1/G$  on larger lattices. We have checked that the data not satisfying the restriction (5.1) behave in a similar way. Furthermore, one can observe the now apparent difference from the asymptotic scaling behavior (4.12), with an indication how this behavior would be slowly achieved on huge lattices (dotted lines). We find that the SD equations describe the data for  $s \leq 0.5$  long before the asymptotic scaling sets on. This allows us to extrapolate the data obtained on achievable lattices to large  $1/G$ , and to interpret them as an evidence for the asymptotic scaling (4.11)–(4.12), expected for the  $\text{GN}_2$  model with nonzero bare mass.

We expect that the discrepancies observed at  $s = 0.6$  and  $0.7$  are due to the truncation, and thus do not indicate any deviation from the asymptotic scaling. This is further supported by the observation that the agreement between the data and the SD equations is improved even at larger  $s$ , if we plot the data for  $am_F/am_0 Z$ , with  $Z$  measured by means of the relation (2.7), and compare them with the SD equation using (4.5) (see Fig. 5). Because the measured values of  $Z$  are consistent with  $Z \rightarrow 1$  for  $G \rightarrow 0$ , as follows also from eq. (4.5), the asymptotic behavior is not changed, and we now see how it is approached even for larger  $s$ .

As a preparation for the studies at  $\beta > 0$ , it is illustrative to test, at  $\beta = 0$ , also the inversion of the SD equations according to eqs. (4.17) and (4.16). The above data for  $am_F$

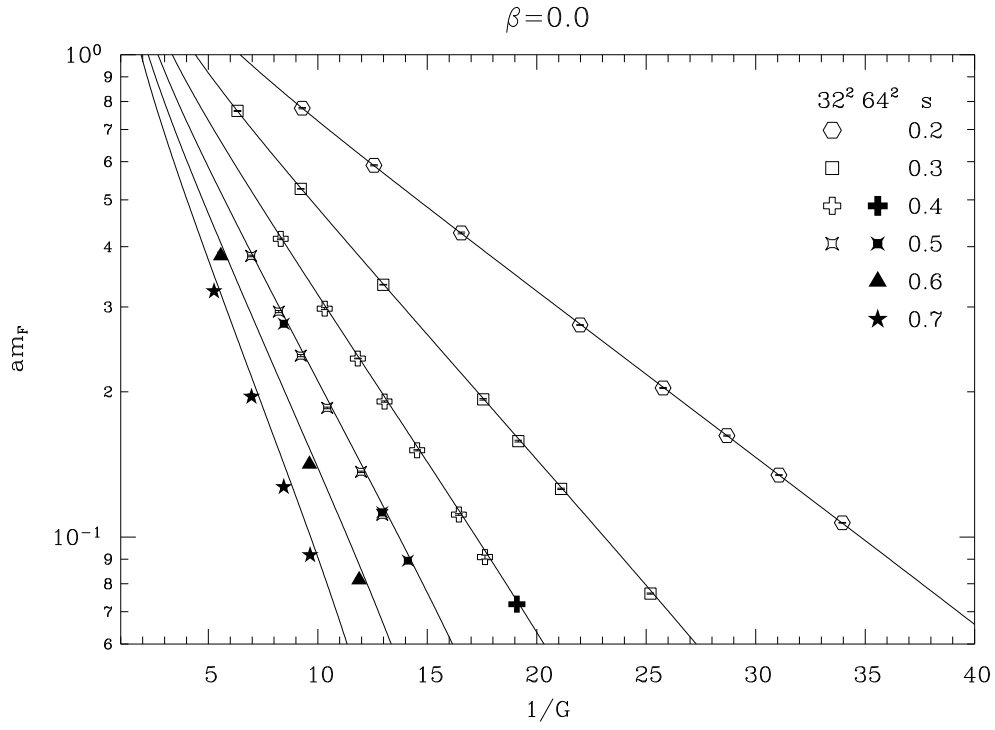


**Figure 3:** The data for  $am_F$  at  $\beta = 0$  for various fixed  $s$  compared with the predictions of the SD equations.

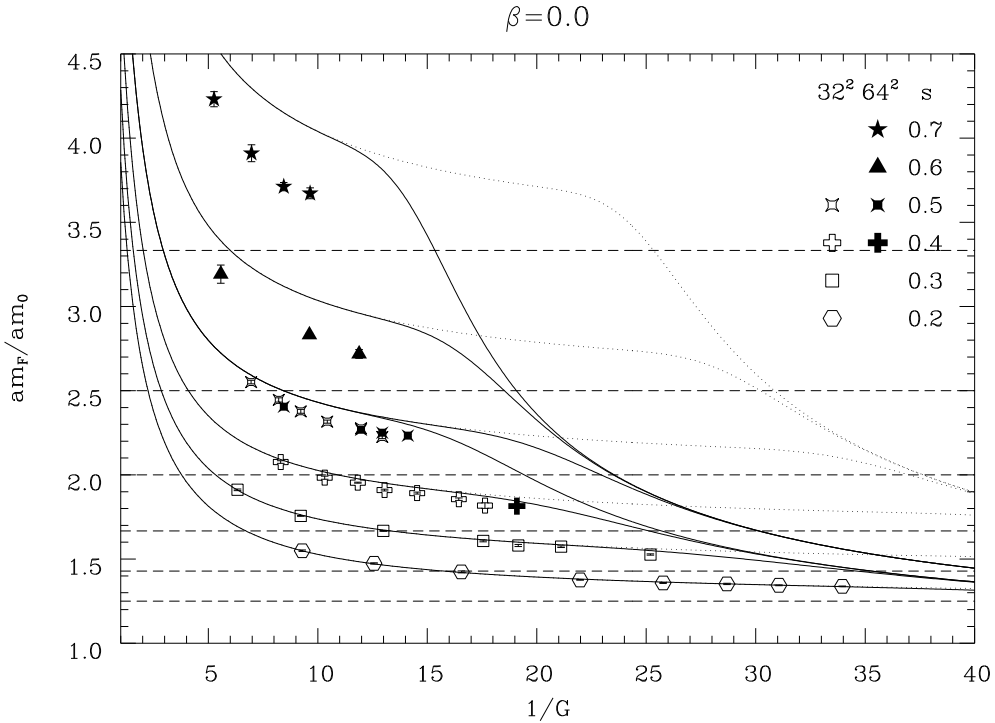


**Figure 4:** The ratio  $am_F/am_0$  at  $\beta = 0$  for various fixed  $s$  compared with the SD equations on  $32^2$  ( $s \leq 0.5$ ) and  $64^2$  ( $s \geq 0.5$ ) lattices (full lines), and  $1024^2$  lattice (dotted lines). The dashed horizontal lines represent the expected asymptotic behavior.

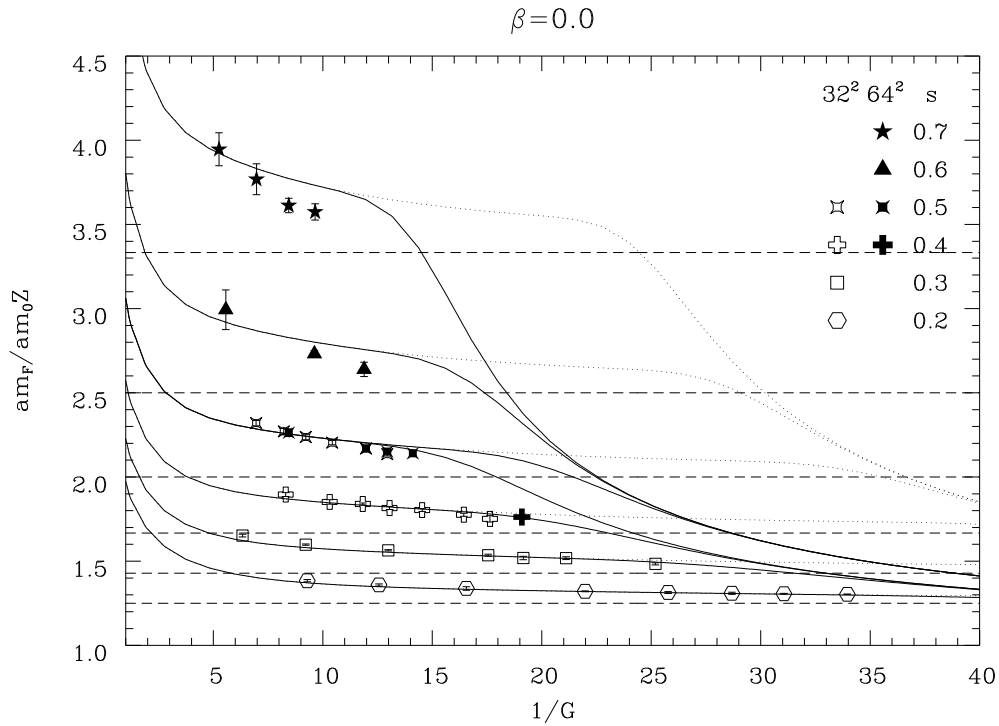


**Figure 5:** As in Fig. 4, but for the ratio  $am_F/am_0 Z$ ,  $Z$  obtained from the fermion propagators (data) and from (4.5) (curves).

has been used as input to these equations, and  $\Gamma(0, G, am_0, V)$  has been obtained by their numerical solution. The results are shown in Fig. 6, where they are compared with the expected value of the coupling  $\tilde{G}(0, G) = G$ . We observe that for a rather large bare mass,  $am_0 = 0.4$ , the agreement is excellent. The fit  $\Gamma(0, G, 0.4, V) = cG^p$  gives, for  $V = 32^2$  and  $64^2$ , results consistent with  $c = p = 1$  (see table 1).

For smaller  $am_0$ , deviations of  $\Gamma$  from the true coupling  $G$  are observable. Of course, these deviations are of the same origin as those in Figs. 3 and 4: they reflect the inaccuracy of the SD equations for larger  $s$ , and thus for smaller  $am_0$ . For a quantitative comparison with the SD equations it is therefore advantageous to perform simulations at not too small  $am_0$ . Nevertheless, even for smaller  $am_0$  the deviations remain small. The degree of agreement between  $\Gamma$  and  $G$  at  $\beta = 0$  can serve at  $\beta > 0$  as an estimate for the accuracy, with which one can determine the effective coupling  $\tilde{G}(\beta, G)$  from the values of  $\Gamma(\beta, G, am_0, V)$  obtained by the inversion of the SD equations.

## 6 Effective four-fermion coupling at $\beta > 0$

The experience gained at  $\beta = 0$  makes it clear that also at  $\beta > 0$  the simulations have to be performed at  $am_0 > 0$ , and that on lattices of affordable sizes there is no chance to observe the asymptotic scaling directly. Therefore, we investigate the scaling behavior of the fermion mass  $am_F$  at  $\beta > 0$  by means of the following strategy:

1. The conjecture that the  $\chi U\phi_2$  model at  $\beta > 0$  belongs to the same universality class as the  $GN_2$  model suggests the use of the same SD equations as at  $\beta = 0$  for the description of the nonasymptotic data for  $am_F$ . The only foreseen difference is the

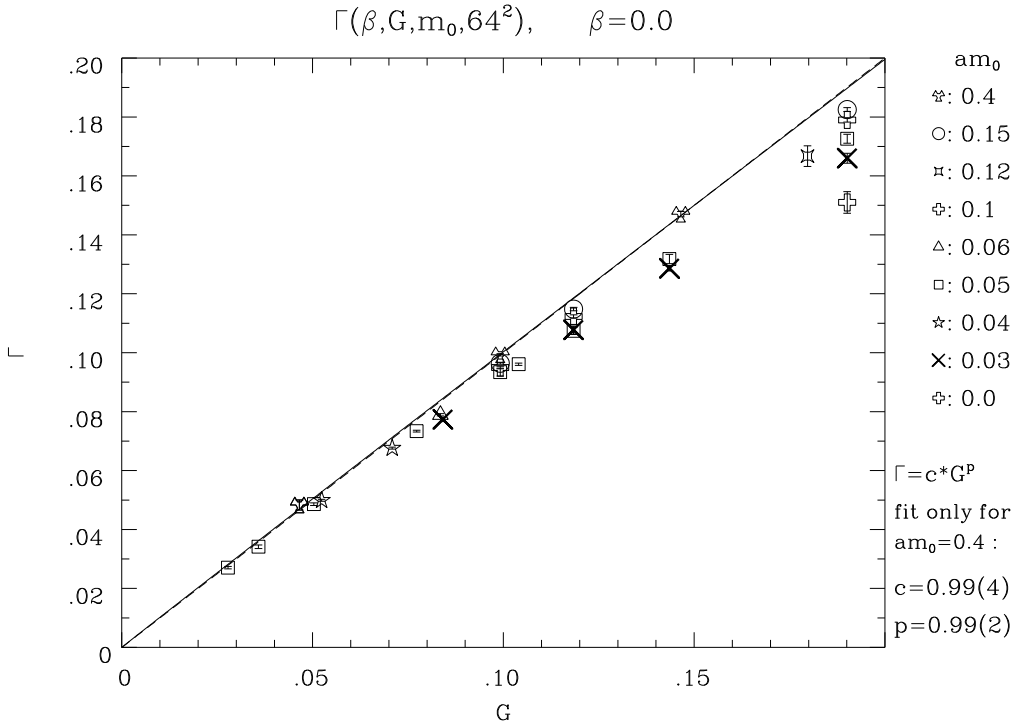


**Figure 6:** The values of  $\Gamma(\beta, G, am_0, V)$  obtained by the inversion of the SD equations at  $\beta = 0$  for  $V = 64^2$ . The full line representing the fit by means of eq. (6.2) to the  $am_0 = 0.4$  data nearly coincides with the diagonal (dashed) line.

value of the effective four fermion coupling  $\tilde{G}(\beta, G)$ , which is not any more a known function (2.3) of  $\kappa$ , but has to be determined from the data. A similar idea was very successful in the earlier study of the universality class of the two-dimensional Yukawa model [9].

2. For each value of  $am_F$ , obtained at some  $\beta$ ,  $G$  and  $am_0$  on a lattice of volume  $V$ , we invert the SD equations (4.16) and (4.17), obtaining  $\Gamma(\beta, G, am_0, V)$ .
3. Of course, in principle the effective coupling should be independent of  $am_0$  and  $V$ . Because of the limited accuracy of the truncated SD equations, some dependence of  $\Gamma(\beta, G, am_0, V)$  on  $am_0$  remains, however. On the basis of the observation that at  $\beta = 0$  the values of  $\Gamma$  and  $G$  are consistent for  $am_0 = 0.4$ , we assume that also at  $\beta > 0$  the values of  $\tilde{G}(\beta, G)$  can be obtained for this  $am_0$ , and define

$$\tilde{G}(\beta, G) = \Gamma(\beta, G, am_0 = 0.4, V). \quad (6.1)$$

This effective four-fermion coupling is  $V$ -independent, provided  $V$  is sufficiently large.

4. At each  $\beta$ , we determine the  $G$ -dependence of  $\tilde{G}(\beta, G)$ , which turns out to be consistent with a power law

$$\tilde{G}(\beta, G) = c(\beta)G^{p(\beta)}. \quad (6.2)$$

5. If  $\tilde{G}(\beta, G)$  were known prior to the numerical calculations of  $am_F$  at  $\beta > 0$ , one would choose the data points so that in the  $(am_0, G)$  plane they lie on lines similar to (4.8), with  $G$  replaced by  $\tilde{G}(\beta, G)$ . The same simple comparison with the expected scaling

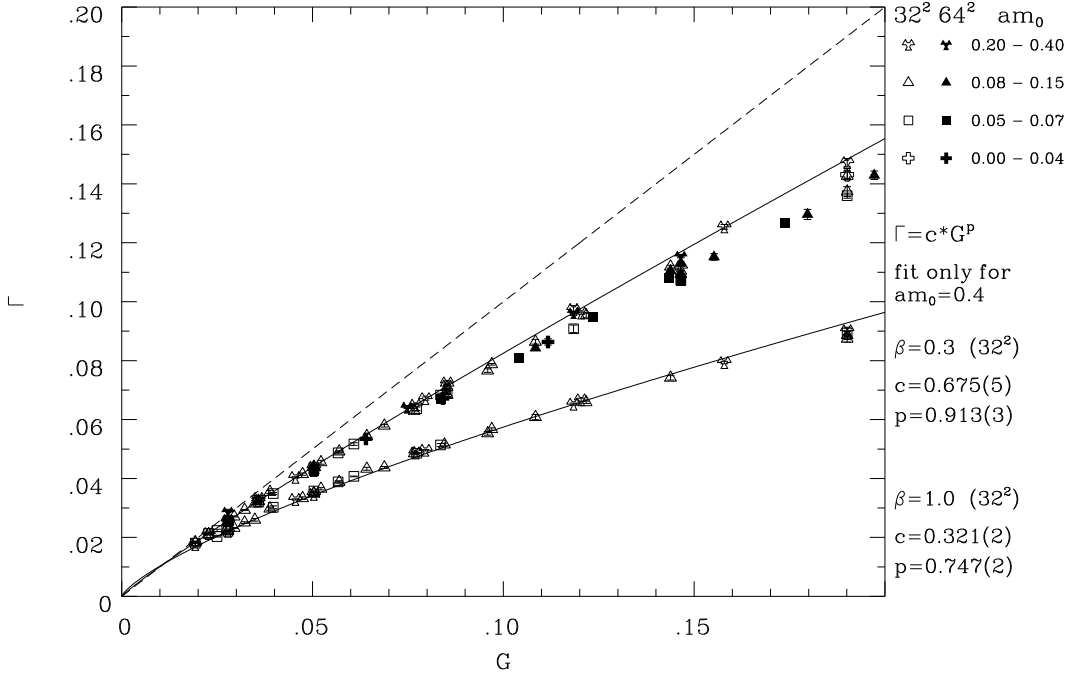


**Figure 7:** The values of  $\Gamma(\beta, G, am_0, V)$  at  $\beta = 0.3$  and  $\beta = 1.0$ . The full lines are fits by means of eq. (6.2) to the  $am_0 = 0.4$  data. They represent the obtained effective coupling  $\tilde{G}(\beta, G)$ .

behavior (4.11), now with  $\tilde{G}(\beta, G)$ , would then be possible. Without this knowledge, we have decided to acquire the data on the same lines of constant  $s$ , eq. (4.8), as at  $\beta = 0$ . As will be explained in the next section, one can then recalculate the predictions of the SD equations with  $\tilde{G}(\beta, G)$  to the lines  $s = \text{const.}$ , and observe the approach to the scaling behavior, though these lines are now less suitable for this purpose.

We have determined  $am_F$  at  $\beta = 0.2, 0.3, 0.5, 0.7, 1.0$  on the  $32^2$  lattice for  $s = 0.2, 0.3, 0.4, 0.5$ , and at  $\beta = 0.3$  also on the  $64^2$  lattice for  $s = 0.4, 0.5, 0.6, 0.7$ . The intervals of the  $G$  and  $am_0$  values have been chosen such that the fermion mass is consistent with the requirement (5.1). As expected, the fermion mass  $am_F$  decreases with increasing  $\beta$  at constant  $G$ , because of the decreasing gauge coupling.

For  $\beta > 1$  the mass  $am_F$  is measurable only in a small  $G$ -interval below or in the vicinity of the dashed line in Fig. 1. Nevertheless, one can see that  $am_F$  is insensitive to this line.

In Fig. 7 we show the results for  $\Gamma(\beta, G, am_0, V)$  at  $\beta = 0.3$  and  $\beta = 1$ . They cluster for each  $\beta$  along, or slightly below a simple curve. This curve is the power law fit (6.2) to the values of  $\tilde{G}(\beta, G)$ , determined according to eq. (6.1) at  $am_0 = 0.4$ . The results for smaller  $am_0$  do not deviate from this curve more than in the  $\beta = 0$  case (Fig. 6). For other  $\beta$  values the results are very similar.

Fits by means of the power law (6.2) describe the data at  $am_0 = 0.4$  very well. In table 1 we present the results for the fit parameters  $c(\beta)$  and  $p(\beta)$ . The indicated errors come from the Minuit fit for  $\tilde{G}(\beta, G)$  by means of eq. (6.2). As the values of  $\tilde{G}(\beta, G)$  result from a data analysis in several steps, these errors are too naive. A more realistic error estimate might be the difference between the results on  $32^2$  and  $64^2$  lattices at  $\beta = 0$ , where we know that these results should be consistent. This suggests the errors of sizes  $\Delta c/c \simeq 0.05$  and

$\beta$	$32^2$		$64^2$	
	$c$	$p$	$c$	$p$
0.0	1.038(7)	1.016(4)	0.99(4)	0.99(2)
0.2	0.767(9)	0.940(5)		
0.3	0.675(5)	0.913(3)	0.62(1)	0.88(1)
0.5	0.512(6)	0.844(4)		
0.7	0.422(3)	0.806(2)		
1.0	0.321(2)	0.747(2)		

**Table 1:** The values of the parameters determining the effective coupling  $\tilde{G}(\beta, G)$  by means of eq. (6.2). See the text for a discussion of the errors.

$\Delta p/p \simeq 0.03$ .

These results demonstrate that the introduction of the effective four fermion coupling  $\tilde{G}(\beta, G)$  by means of the SD equations is sensible. In other words, one can find such a function  $\tilde{G}(\beta, G)$ , that the data is consistent with the SD equations when  $\tilde{G}(\beta, G)$  is used as a coupling. Assuming now that this is true also at smaller  $G$  and  $am_0$ , i.e. beyond the intervals we could investigate, we can deduce the scaling behavior of  $am_F$  with  $\tilde{G}(\beta, G)$  from these SD equations.

The power law dependence (6.2) of  $\tilde{G}(\beta, G)$  on  $G$  is questionable for very small  $G$  because of the singular behavior at  $G = 0$ , and probably should not be trusted there. K.-I. Kondo has investigated in the continuum a model quite similar to the  $\chi U\phi_2$  model, both in  $d = 4$  [7] and  $d = 2$  [10]. Recently, he has obtained in  $d = 2$ , by solving the SD equations for the full  $\chi U\phi_2$  model, the effective four-fermion coupling  $\tilde{G}$  as a series in  $G$  [10]. This would contradict (6.2). We have checked that our results for  $\tilde{G}$  can be described by a polynomial in  $G$ , too, but the coefficients of the higher powers of  $G$  are large and unstable, and such an analytic description is therefore of little use.

## 7 Scaling behavior at $\beta > 0$

According to the results presented in the previous section, the SD equations with  $G$  replaced by  $\tilde{G}(\beta, G)$  describe the data for  $am_F$  for larger  $am_0$  values. These equations predict also the behavior of  $am_F/am_0$  as  $\tilde{G}$  and  $am_0$  approach zero along the lines

$$\frac{1}{r(\tilde{G})} am_0(\tilde{G}, \tilde{s}) = (1 - \tilde{s}) \frac{\pi F}{2} e^{-\frac{\pi F^2 \tilde{s}}{8\tilde{G}}}, \quad \tilde{s} = \text{const.}, \quad (7.1)$$

in the  $(am_0, \tilde{G})$  plane. Along these lines the asymptotic scaling behavior is analogous to (4.11),

$$am_F = \frac{\pi}{2} e^{-\frac{\pi \tilde{s}}{8\tilde{G}}}, \quad \frac{am_F}{am_0} = \frac{1}{1 - \tilde{s}}. \quad (7.2)$$

This is the same scaling behavior as in the  $\text{GN}_2$  model with  $am_0 \geq 0$ , when  $G$  is replaced by  $\tilde{G}$ . From eqs. (2.3), (2.4) and (6.2) it follows that  $\tilde{G}(\beta, G) \rightarrow 0$  as  $\kappa \rightarrow \infty$ . The successful analysis of the data for  $am_F$  at  $\beta > 0$  by means of the SD equations with  $\tilde{G}(\beta, G)$  is thus an indication that the  $\chi U\phi_2$  model at  $\beta > 0$  belongs to the same universality class as the  $\text{GN}_2$

model, when the critical line  $\kappa = \infty$  is approached. In the chiral limit, the scaling behavior predicted by the SD equations with  $\tilde{G}(\beta, G)$  is

$$am_F \propto e^{-\frac{\pi}{8\tilde{G}}} = e^{-\frac{\pi}{8cG^p}}, \quad (7.3)$$

to be compared with (2.5) at  $\beta = 0$ .

Of course, our data with rather large  $am_0$  and  $am_F$  do not show directly this asymptotic scaling, but only an approach to it, as predicted by the SD equations. To illustrate this, in Fig. 8 we compare the data obtained on lines  $s = \text{const}$ , (4.8), with the predictions for these lines of the SD equations with  $\tilde{G}(\beta, G)$ . As in Fig. 5, we plot the ratio  $am_F/am_0$ , and the full lines are the numerical solutions of the SD equations with  $\tilde{G}(\beta, G)$ . As at  $\beta = 0$ , Fig. 5, we observe a very good agreement for smaller  $s$  (larger  $am_0$ ), whereas at larger  $s$  at least a qualitative behavior of the data is reproduced.

The data at  $\beta > 0$  has been taken on the lines (4.8), which are not as convenient as the lines (7.1) would be. Nevertheless, one can obtain the asymptotic behavior on the lines (4.8) as follows: comparing eqs. (4.8) and (7.1) we eliminate  $am_0$ , obtaining a relation between the pairs of parameters  $(G, s)$  and  $(\tilde{G}, \tilde{s})$ ,

$$(1-s)e^{-\frac{\pi}{8G}s} = (1-\tilde{s})e^{-\frac{\pi}{8\tilde{G}}\tilde{s}}. \quad (7.4)$$

Using this relation in eq. (7.2) we obtain for small  $G$  (i.e. setting  $r = F_\mu = 1$ )

$$am_F = \frac{\pi}{2} \frac{1-s}{1-\tilde{s}(\beta, G, s)} e^{-\frac{\pi}{8G}s}, \quad (7.5)$$

where  $\tilde{s}$  is now understood as a function  $\tilde{s}(\beta, G, s)$ .

This function  $\tilde{s}(\beta, G, s)$  can be determined at each  $\beta$  from the now known  $G$ -dependence (6.2) of  $\tilde{G}(\beta, G)$ . The results at  $\beta = 0.3$  for various fixed values of  $am_0$  are shown in Fig. 9. We observe that, for small  $s$ , the values of  $\tilde{s}$  are nearly independent of  $am_0$ , and thus of  $G$ . This explains why the  $\tilde{G}$ -dependence of the data in Fig. 8 looks very similar to the  $G$ -dependence of the data at  $\beta = 0$ , fig. 5, up to a – nearly constant – factor  $(1-s)/(1-\tilde{s})$ . This similarity is easily observable [11], as no determination of  $\tilde{s}(G, s)$  is required, and thus constitutes a simpler comparison of  $am_F$  in the  $\chi U\phi_2$  model at  $\beta > 0$  with the predictions of the SD equations with  $\tilde{G}$ .

The observed agreement between the nonasymptotic data and the SD equations of the  $\text{GN}_2$  model with  $\tilde{G}$  suggests that also the asymptotic scaling behavior of the  $\chi U\phi_2$  model at  $\beta > 0$  is described by these equations, and the model thus belongs to the same universality class. But, of course, this is only a conjecture, as the region investigated is limited by the applicability of the truncated SD equations, as well as by the constraints of a numerical approach.

## 8 Conclusions and discussion

By introducing an effective four-fermion coupling  $\tilde{G}(\beta, G)$  in the  $\chi U\phi_2$  model at  $\beta > 0$  we have found that – within the limits of a numerical approach – this model is described by the same SD equations as the chiral  $\text{GN}_2$  model with coupling  $G$  replaced by  $\tilde{G}$ . The scaling behavior, when  $\tilde{G} \rightarrow 0$ , is thus the same as in the  $\text{GN}_2$  model in the  $G \rightarrow 0$  limit. This is an indication that the  $\chi U\phi_2$  model belongs to the universality class of the  $\text{GN}_2$  model.

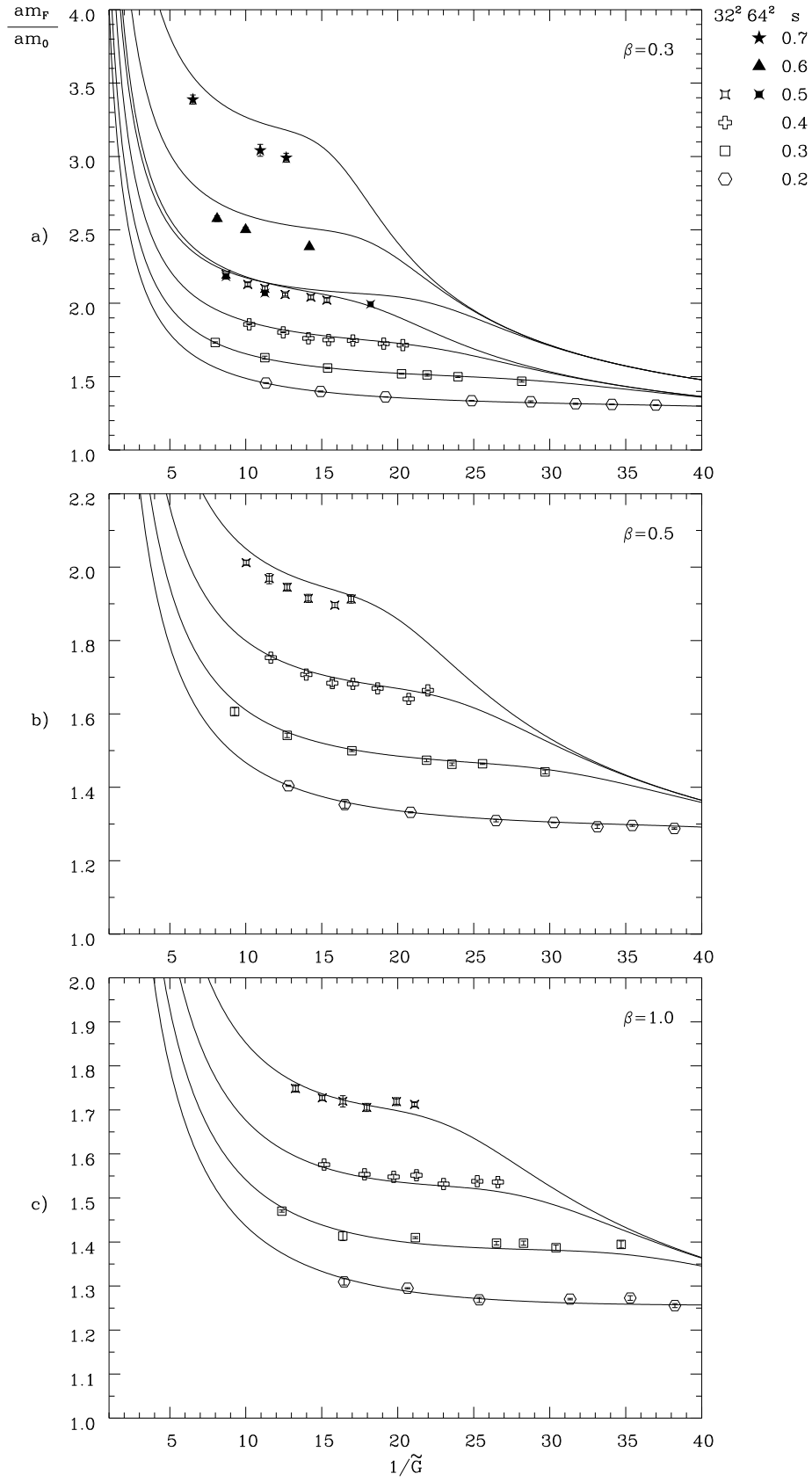


**Figure 8:** The ratio  $am_F/am_0$  along the lines  $s = \text{const.}$ , eq. (4.8), at  $\beta = 0.3, 0.5$  and  $1.0$ . The full lines are predictions of the SD equations with  $\tilde{G}(\beta, G)$  described by eq. (6.2).



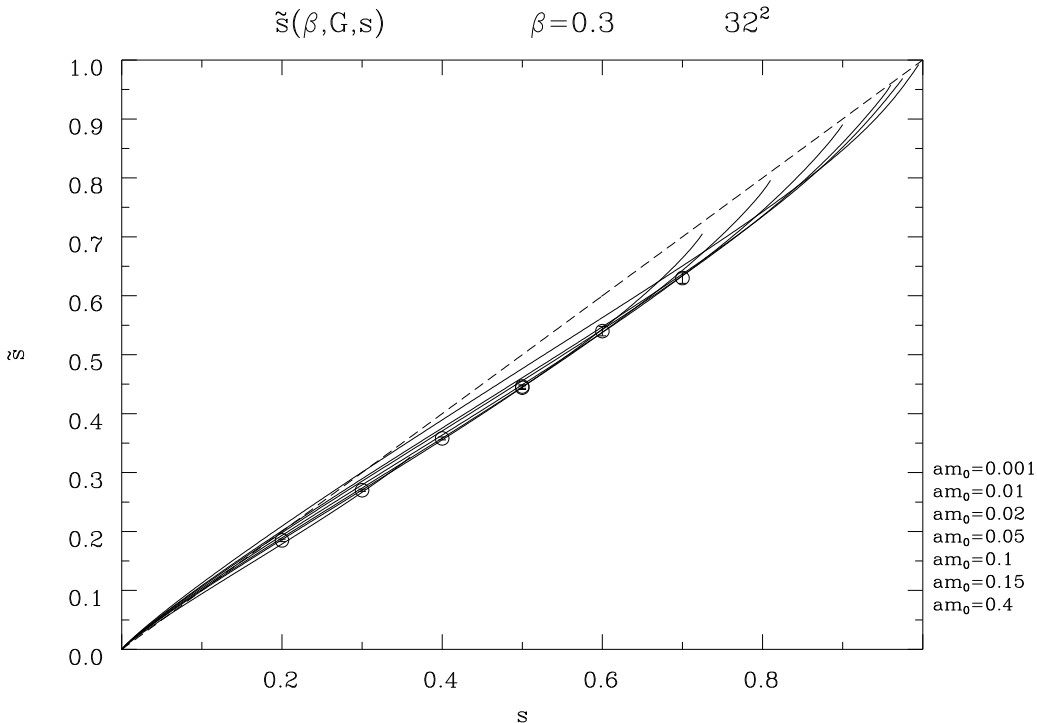


**Figure 9:** The values of  $\tilde{s}(\beta, G, s)$  at  $\beta = 0.3$  for fixed  $am_0$ , determining  $G$  by using eq. (4.8). The curves are independent of the lattice volume. The data are from Ref. [11].

From this we tentatively conclude that the  $\chi U\phi_2$  model is nonperturbatively renormalizable and, though defined on the lattice, possesses a well defined continuum limit. It is thus an example of a strongly coupled gauge theory with continuous chiral symmetry, in which the fermion mass is generated dynamically and the massive fermions are not confined. At least in two dimensions the shielded gauge mechanism of fermion mass generation, suggested in Ref. [1], exists. The  $\chi U\phi_2$  model nicely illustrates this mechanism.

On the other hand, the  $\chi U\phi_2$  model is presumably too simple to provide useful hints how to approach the  $d = 4$  case. Our results suggest that the complexity of the  $\chi U\phi_2$  model, and the composite structure of the fermion  $F = \phi^\dagger \chi$ , are effects not surviving the continuum limit. The possibility of describing the scaling properties in terms of the van der Waals force, represented by the effective four-fermion coupling, shows that in the renormalized theory the inner structure of the fermion, acquiring its mass dynamically, is irrelevant.

The study of the renormalizability properties of the strongly coupled  $\chi U\phi_2$  model has been made relatively easy in  $d = 2$  by its neighborhood to the well understood  $GN_2$  model. Still, the applicability of the SD equations long before the onset of asymptotic scaling has been a surprise, even in the  $GN_2$  model. The use of these equations has been crucial, since an asymptotic scaling behavior is evidently not obtainable in numerical simulations, and a method of extrapolation to the scaling limit, and to the limit of chiral symmetry, is required.

A plausible explanation why the  $\chi U\phi_2$  model is well described by the SD equations of the  $GN_2$  model might be as follows: Integrating out the gauge and scalar field, one ends up with a pure fermionic theory with many multi-fermion couplings. These fermions correspond to our fermions  $F$ , as in the  $\beta = 0$  limit. The universality of multi-fermion couplings in  $d = 2$ , observed e.g. in the studies of the  $d = 2$  Yukawa model [9], suggests that the four-fermion coupling is dominant and sufficient to describe the data.

Provided that the  $\chi U\phi_2$  model at  $\beta > 0$  really belongs to the  $GN_2$  universality class, the most interesting question left is the dependence of the effective four-fermion coupling  $\tilde{G}$  on  $G$  and  $\beta$ . We hope that our data for  $\tilde{G}(\beta, G)$  will stimulate its theoretical investigation.

## Acknowledgments

We thank E. Focht, M. Göckeler, K.-I. Kondo, M.-P. Lombardo, and P. Rakow for discussions, and M. M. Tsypin for drawing our attention to Refs. [2]. The computations have been performed on the Cray-YMP of HLRZ Jülich. The work has been supported by the BMBF and DFG.

## References

- [1] C. Frick and J. Jersák, Phys. Rev. D **52**, 340 (1995).
- [2] C. G. Callan, R. Dashen, and D. Gross, Phys. Rev. D **16**, 2526 (1977);  
S. Raby and A. Ukawa, Phys. Rev. D **18**, 1154 (1978).
- [3] W. Franzki, C. Frick, J. Jersák, and X. Q. Luo, Nucl. Phys. B **453**, 355 (1995).
- [4] W. Franzki and J. Jersák, Tricritical point in strongly coupled U(1) gauge theory with fermions and scalars, (Proceedings of Lattice '95, Melbourne); preprint HLRZ 54/95, hep-lat/9509038.
- [5] A. Ali Khan *et al.*, Phys. Rev. D **51**, 3751 (1995).
- [6] I.-H. Lee and R. E. Shrock, Phys. Rev. Lett. **59**, 14 (1987).
- [7] K.-I. Kondo, The gauged Thirring model, preprint CHIBA-EP-93, HLRZ 1/96.
- [8] S. Grunewald, E.-M. Ilgenfritz, and M. Müller-Preussker, Z. Phys. C **33**, 561 (1987);  
F. Karsch, M. L. Laursen, T. Neuhaus, and B. Plache, Nucl. Phys. B **406**, 825 (1993).
- [9] A. K. De *et al.*, Phys. Lett. B **308**, 327 (1993);  
E. Focht, W. Franzki, J. Jersák, and M. A. Stephanov, Nucl. Phys. B **429**, 431 (1994).
- [10] K.-I. Kondo, private communication.
- [11] W. Franzki, J. Jersák, and R. Welters, Gauge invariant generalization of the 2D chiral Gross-Neveu model, (Proceedings of Lattice '95, Melbourne), preprint HLRZ 55/95, hep-lat/9509042.